A Genetic Screen for Neurite Outgrowth Mutants in *Caenorhabditis elegans* Reveals a New Function for the F-box Ubiquitin Ligase Component LIN-23

Nehal Mehta, Paula M. Loria and Oliver Hobert[1]

Department of Biochemistry and Molecular Biophysics, Center for Neurobiology and Behavior, Columbia University, College of Physicians and Surgeons, New York, New York 10032

Manuscript received July 22, 2003
Accepted for publication October 14, 2003

ABSTRACT

Axon pathfinding and target recognition are highly dynamic and tightly regulated cellular processes. One of the mechanisms involved in regulating protein activity levels during axonal and synaptic development is protein ubiquitination. We describe here the isolation of several *Caenorhabditis elegans* mutants, termed *eno* (*e*ctopic/*e*rratic *n*eurite *o*utgrowth) mutants, that display defects in axon outgrowth of specific neuron classes. One retrieved mutant is characterized by abnormal termination of axon outgrowth in a subset of several distinct neuron classes, including ventral nerve cord motor neurons, head motor neurons, and mechanosensory neurons. This mutant is allelic to *lin-23*, which codes for an F-box-containing component of an SCF E3 ubiquitin ligase complex that was previously shown to negatively regulate postembryonic cell divisions. We demonstrate that LIN-23 is a broadly expressed cytoplasmically localized protein that is required autonomously in neurons to affect axon outgrowth. Our newly isolated allele of *lin-23*, a point mutation in the C-terminal tail of the protein, displays axonal outgrowth defects similar to those observed in null alleles of this gene, but does not display defects in cell cycle regulation. We have thus defined separable activities of LIN-23 in two distinct processes, cell cycle control and axon patterning. We propose that LIN-23 targets distinct substrates for ubiquitination within each process.

AXONS are extraordinarily dynamic cellular structures. During development, the growth cone of an axon is steered toward its target area through the concerted action of intrinsic and extrinsic molecular cues. The responsiveness of a growth cone to specific extracellular cues can significantly change along the path that an axon takes to reach its target. Upon reaching its target area and achieving target recognition, a growth cone is transformed into a synapse. A mature synapse undergoes further dynamic remodeling, a process that is dependent on electrical activity at the synapse. Post-translational protein modification through ubiquitination has been found to affect each of these dynamic cellular processes (Hegde and DiAntonio 2002; Murphey and Godenschwege 2002).

The ubiquitination machinery is composed of several proteins (Hegde and DiAntonio 2002). Ubiquitin, a 76-amino-acid protein, is initially activated by an E1 enzyme. It is then transferred to the E2-conjugating enzyme, which associates with an E3 ligase complex to transfer ubiquitin to the eventual target protein. Several classes of E3 ubiquitin ligase complexes exist. One of these, the SCF E3 ubiquitin ligase complex, consists of four proteins, an *S*kp1-like protein, a *C*ullin, an *F*-box protein, and a RING domain containing Rbx-like protein (Craig and Tyers 1999; Joazeiro and Weissman 2000). The SCF ligase complex is constitutively active but recognizes only phosphorylated substrates. Its substrate specificity is determined by its F-box protein subunit. The large number of F-box proteins in databases prompted the "F-box hypothesis," which posits that specific substrates are recruited through defined F-box proteins (Bai *et al.* 1996). Consistent with this notion, F-box proteins are bipartite in composition, containing an F-box domain required for interaction with the core ligase complex and other protein-protein interaction motifs that may bind and recruit protein substrates (Craig and Tyers 1999; Kipreos and Pagano 2000).

The consequences of protein ubiquitination on a molecular level are diverse. Originally identified as a tag that targets proteins to the degradation apparatus (Hochstrasser 1996), more recent studies have emphasized the involvement of protein ubiquitination in a variety of other cellular processes such as intracellular protein trafficking, transcriptional control, and DNA repair (Bach and Ostendorff 2003; Hicke and Dunn 2003).

The cellular and organismal consequences of protein ubiquitination have begun to be elucidated. Several connections between ubiquitination and neuronal development were made with the use of genetically tractable model organisms. The identification of Drosophila *bendless* as an E2-conjugating enzyme provided the first in-

[1]*Corresponding author:* Columbia University, College of Physicians and Surgeons, 701 W. 168th St., HHSC 724, New York, NY 10032. E-mail: or38@columbia.edu

sights into the importance of ubiquitination as a regulatory mechanism for axon pathfinding (Thomas and Wyman 1982; Muralidhar and Thomas 1993). A surprising feature of the *bendless* mutant phenotype is its high selectivity, exemplified through *bendless* affecting only one of several connections in the giant fiber system (Thomas and Wyman 1982). More recently, specific axonal cues were found to be controlled through protein ubiquitination. Axon pathfinding at the midline in Drosophila requires the Robo axon guidance receptor whose cell surface expression is downregulated by commissureless (Comm), a lysosomal endocytotic sorting protein (Keleman *et al.* 2002; Myat *et al.* 2002). Ubiquitination of Comm by the ubiquitin ligase Nedd4 is thought to be required for Comm to traffic the Robo receptor from the plasma membrane to endosomes (Myat *et al.* 2002). Ubiquitinated Comm may also have similar roles in downregulating cell surface proteins during neuromuscular synapse formation (Wolf *et al.* 1998; Hegde and DiAntonio 2002). In vertebrates, the axon guidance cue netrin elicits changes in the ubiquitination state of proteins in isolated retinal growth cones (Campbell and Holt 2001) and, furthermore, the Netrin receptor DCC is subjected to ubiquitin-mediated protein degradation (Hu *et al.* 1997), thus illustrating the widespread use of ubiquitination in distinct axon pathfinding events.

The importance of ubiquitination extends from axon outgrowth and target recognition to the processes of synaptic growth and synaptic plasticity. In Drosophila, overexpression of the deubiquitinating enzyme, *fat facets,* causes defects in synaptic size and strength (DiAntonio *et al.* 2001). An enhancer of *fat facets*, *highwire*, displays similar defects. *Highwire* encodes a RING finger protein and has been proposed to be a member of a family of E3 ubiquitin ligases (Wan *et al.* 2000). Its worm homolog *rpm-1* has also been implicated in synaptogenesis (Schaefer *et al.* 2000; Zhen *et al.* 2000). Another link between ubiquitination and synaptic transmission is provided by the observation that postsynaptic clustering of the *Caenorhabditis elegans* glutamate receptor *glr-1* is regulated by ubiquitination *in vivo*; mutations that decrease the ubiquitination of GLR-1 lead to altered locomotion behavior in a manner that is consistent with increased synaptic strength (Burbea *et al.* 2002). Studies in Aplysia have further underscored the importance of ubiquitination in synaptic plasticity, an effect that is exerted through the regulated degradation of defined intracellular signaling components such as the regulatory subunit of protein kinase A and the transcription factor C/EBP (Hegde *et al.* 1993; Hegde *et al.* 1997; Yamamoto *et al.* 1999).

In this article, we describe a novel aspect of ubiquitin function in the nervous system, namely its role in terminating axon outgrowth. We show that LIN-23, an F-box-containing component of an SCF E3 ubiquitin ligase complex, is required cell autonomously for normal axonal outgrowth. Our newly isolated *lin-23* allele furthermore uncouples roles of *lin-23* in axonal outgrowth and cell cycle regulation. Our studies therefore provide an example of the diversity of cellular processes in which a single ubiquitin ligase is involved.

MATERIAL AND METHODS

Strains: The following strains were used: N2 *C. elegans* wild-type var. Bristol; RW7000 *C. elegans* wild type, RW subclone of Bergerac BO; CB4856, isolated from a pineapple field in Hawaii in 1972 by L. Hollen; ET003 *lin-23(e1925)II/dpy-10(e128)*; ET009 *lin-23 (e1521)II/dpy-10(e128)*; ET012 *lin-23(e1883)II/mnC1*; ET032 *lin-23(rh194)II/mnC1*; ET041 *lin-23(rh294)II/bli-2(e768)*; ET068 *lin-23(rh293)II/bli-2(e768)*; ET073 *lin-23(m731), unc-4(e120)II/ mC6*; NJ582 *cul-1(e1756)/unc-69(e587)III*; CB845 *unc-30(e191)III*; GS1063 *rol-6 (e187)II*; MT301 *lin-31(n301)II*; NM1448 *rpm-1 (js410)V*; CB61 *dpy-5(e61)I*; CB184 *dpy-13(e184)IV*; SP552 *mnDf39 unc-4(e120)/mnC1;dpy-10(e128);unc-52(e444)II*;SP543 *mnDf30 unc-4(e120)/mnC1dpy-10(e128)unc-52(e444)II*;CB2196 *daf-4 (e1364ts)unc-32(e189)III*;OH110 *lim-6(nr2073)X*;andGS1081 *sel-10(ar41)him-5(e1490)*.

The following reporter transgenes were used (all chromosomally integrated): *oxIs12*, expresses *unc-47::gfp* (McIntire *et al.* 1997); *uIs25*, expresses *mec-18::gfp* (Wu *et al.* 2001); *jsIs42*, expresses *unc-4::snb-1::gfp* (Nonet 1999); *otIs92*, expresses *flp-10::gfp* (derived from an extrachromosomal array kindly provided by C. Li); *mgIs18*, expresses *ttx-3::gfp* (Altun-Gultekin *et al.* 2001); and *nuIs63*, expresses *ceh-24::gfp* (Harfe and Fire 1998), kindly provided by J. Kaplan.

DNA constructs: For the transcriptional reporter *lin-23prom::gfp*, 2.2 kb of sequence 5′ to the start codon of *lin-23* was amplified from N2 wild-type genomic DNA (upstream primer sequence, 5′-GAATAGAGCGGATGTTCG-3′; upstream nested primer sequence, 5′- CCAAATTTGCCTCTGATTCCG-3′; *gfp* fusion primer, 5′-ctagagtcgacctgcaggc TTAATGTCCTG AATTAAATGG-3′). The 3.0-kb amplicon was PCR fused to *gfp* using a previously described protocol (Hobert 2002). For the translational reporter *lin-23::gfp*, the same upstream primers were used, yet the fusion to *gfp* was at the 3′ end of the *lin-23* locus so as to include all exons and introns of *lin-23* (*gfp* fusion primer, 5′- ctagagtcgacctgcaggcTGGGCCACCATC TGGCAT-3′). *lin-23::gfp* constructs that contained the *ot1* or *rh294* mutations (P610S and Q12Stop, respectively) were constructed using the same primers for the PCR fusion reaction. The amplicons were derived from *ot1* or *rh294* homozygous mutant DNA. All constructs were injected at 20 ng/μl, together with 50 ng/μl *rol-6(d)* and 30 ng/μl Stratagene (La Jolla, CA) pBluescript II SK+, to bring the DNA concentration to a total of 100 ng for stable array formation.

The *lin-23* full-length cDNA clone yk784a08 was obtained from the Kohara expressed sequence tag collection. The amplified 2.1-kb cDNA was subcloned into *Sma*I/*Kpn*I restriction sites of *unc-47::MCS*. The cDNA was sequenced after subcloning and a single-amino-acid change was found and corrected back to wild type. *unc-47::MCS* was created by subcloning a 1.2-kb region of the *unc-47* promoter into *Pst*I/*Bam*HI sites of pPD95.75. The *gfp* coding region was then replaced with a multiple cloning site (MCS).

Scoring neuroanatomy: Neuroanatomy was scored under a Zeiss Axioplan 2 microscope equipped with a Hamamatsu Orca CCD digital camera using Openlab as image processing software. Neurons were visualized with *gfp* markers, listed above,

or by DiI filling, using a previously described protocol (Hedgecock *et al.* 1985).

Genetic screen and mapping: Three independent screens were performed. In screens 1 and 3, *oxIs12* animals were mutagenized with EMS and 3620 haploid genomes were screened. In screen 2, an *unc-30(e191); oxIs12* strain was mutagenized to prevent D-type motor neurons from obscuring the AVL and DVB axons. In this screen, 1700 haploid genomes were screened. In each screen, five F_1 progeny each were placed onto single plates and allowed to self-fertilize at 25° until their progeny had almost entirely starved out the plate. The entire population was washed off with M9 medium, mounted onto coverslips, and examined under a Zeiss Axioplan 2 microscope for defects in DVB and AVL axon morphology. To isolate homozygous animals from populations in which we noted animals with mutant phenotypes, we blindly singled out 12 animals per population and assessed whether any of those would throw a brood with at least a 20% penetrant mutant phenotype. Animals from these plates were again singled out to confirm that each one would throw >20% mutant animals. Animals were then backcrossed multiple times. Upon backcrossing we noted that one mutant strain, OH2224, which displayed a 96% penetrant AVL/DVB axon defect, contains two separable mutations, each of which alone gave only a lowly penetrant mutant phenotype. We did not pursue this mutant any further.

For genetic mapping, a combination of three-factor, deficiency, sequence-tagged site (STS; using RW7000 as a mapping strain; Williams *et al.* 1992), and single-nucleotide polymorphism (SNP; using CB4856 as a mapping strain) methods were used. *ot1* was initially mapped onto LGII between *stP101* and *maPI* using RW7000. A three-factor cross between *lin-31 (n301)rol-6(e187)* and *ot1; oxIs12* produced 6/21 lin-non-rol animals and 18/23 rol-non-lin animals that retained *ot1*. SNP mapping with the triple-mutant strain *lin-31(n301)ot1rol-6 (e187);oxIs12* and the *Hawaiian* strain CB4856 resulted in the identification of 1/114 recombinants that retained *ot1* and recombined within the genomic region defined by cosmid C32D5. Deficiency analysis indicated that *mnDf30* [−0.9 to −0.21 map units (MU)] failed to complement *ot1*, but *mnDf39* (−0.4 to −0.21 MU) complemented *ot1*. Since *mnDf39* is contained within the *mnDf30* deficiency, further mapping of *mnDf39* dead embryos indicated that the left-hand boundary of the deficiency is between SNPs on T25D10 and K03H9. Thus, the *ot1* mutation was narrowed down to a 62-kb region covered by five cosmids from C32D5 to K03H9. *ot2* was mapped between the *Hawaiian* strain CB4856 SNP markers on W03D8 (−5.6 MU) and VF39H2L (2.9 MU) on LGI. *ot3* was mapped between the RW7000 STS markers *stP156* (−5.33 MU) and *stP103* (−1.35 MU) on LGX. *ot4* was linked to LGII through crossing with *lin-31(n301)rol-6(e187)II*. Lin-rol animals were picked in the F_2 generation and the progeny were scored for axonal outgrowth defects similar to *ot4*. In total, 0/20 linrol animals showed axonal outgrowth defects. *ot6* was initially mapped between the *bP1* (3.15 MU) and *stP6* (6.0 MU) STS markers. On LGV a three-factor cross between *ot6* and *unc-42lin-25* gave 7/12 unc-non-lin recombinants that retained *ot6*. *ot8* was first mapped onto LGIII through SNP mapping and through three-factor crossing between *daf-4* (−1.46 MU) and *unc-32* (0.0 MU). *ot7* was linked onto LGIV by crossing it with *dpy-13(e184)IV*. Dpy animals were picked in the F_2 generation and the progeny were scored for axonal outgrowth defects. In total, 0/10 F_2 dpy animals showed axonal outgrowth defects. *ot9* was placed on LGX through its cosegregation with the X-linked *oxIs12* marker. *ot40* was initially mapped between Hawaiian SNPs on W03D8 (−5.6 MU) and T22A3 (5.0 MU) onto LGI and then to the left of *dpy-5(e61)* (0 MU).

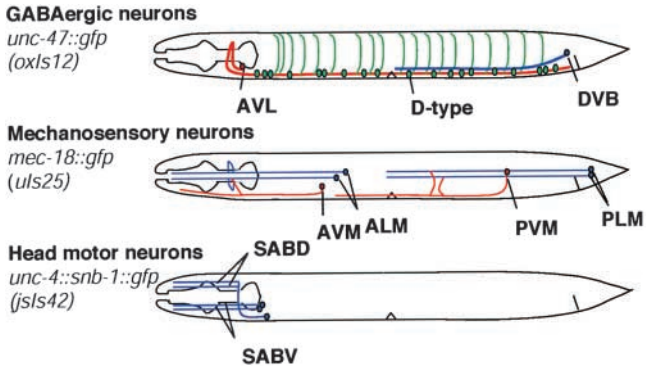

Figure 1.—Schematic of a selection of the neurons tested for axonal and cell proliferation defects. The *oxIs12* transgene (McIntire *et al.* 1997) was used to visualize the GABAergic nervous system, *uIs25* (Wu *et al.* 2001) was used to observe the touch sensory neurons, and *jsIs42* (Nonet 1999) was used to assess the SAB motor neurons. *oxIs12* and *jsIs42* show a broader expression pattern; only neurons of interest are shown here.

RESULTS

A screen for mutants that affect axon anatomy of the AVL and DVB motor neurons: The complete set of GABAergic neurons in the nervous system of *C. elegans* can be labeled with *oxIs12*, a chromosomally integrated transgene expressing *gfp* under the control of the promoter for the GABA transporter *unc-47* (McIntire *et al.* 1997; Figure 1). Various forward and reverse genetic approaches have been used in the past to define genes that affect cell fate determination and axon outgrowth of these GABAergic neurons (McIntire *et al.* 1992, 1993; Jin *et al.* 1994; Eastman *et al.* 1999; Hobert *et al.* 1999; Hammarlund *et al.* 2000; Huang *et al.* 2002). We have previously shown that loss of the LIM homeobox gene *lim-6* causes developmental and axonal defects of the GABAergic ventral cord motor neurons AVL and DVB (Hobert *et al.* 1999; Figure 2A). Of the multiple types of neurons in which *lim-6* is expressed, only the axon anatomy of the AVL and DVB motor neurons is affected by loss of *lim-6* function. In contrast, genes such as *unc-34*, *unc-44/ankyrin*, *unc-61*, *unc-71*, and *unc-76* affect axon anatomy of AVL and DVB (data not shown) as well as of many other if not all neurons of the nervous system (Hedgecock *et al.* 1987; McIntire *et al.* 1992; Antebi *et al.* 1997). Animals carrying mutations in these pleiotropically acting genes hence display obvious morphological, locomotory, and reproductive defects.

To identify genes that like *lim-6* affect axon outgrowth of AVL and DVB in a cell-specific manner, we sought to undertake a genetic screen that would prevent the isolation of genes that affect broad aspects of neuronal development. To this end, we mutagenized animals in which the GABAergic nervous system is labeled with *gfp*, picked five F_1 progeny per plate from the mutagenized P_0 generation, and allowed these animals to produce

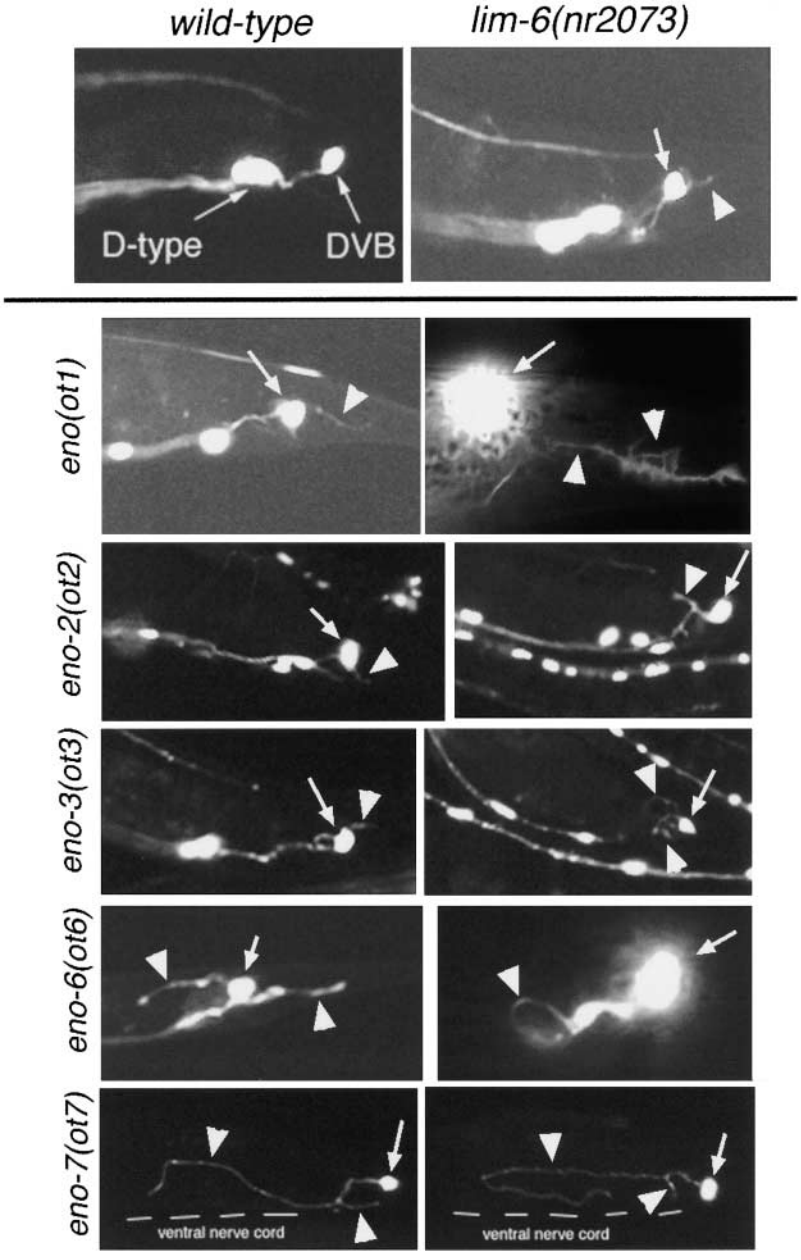

FIGURE 2.—DVB/AVL anatomical defects in *eno* mutants. Anatomy of the GABAergic neurons in a selected number of *eno* mutants is shown. See Table 1 for quantification of defects. For comparison, the previously described *lim-6* mutant phenotype is shown (HOBERT *et al.* 1999). Neurons are visualized with the *oxIs12* transgene. Arrows point to the DVB cell body and arrowheads to defects. More anteriorly located cell bodies are those of the D-type motorneurons (see wild type, left). An extra arrowhead in *eno(ot1)* (right) points to the branched nature of the ectopic axon; as demonstrated in Figure 5, this tail axon is not an ectopic sprout from DVB but rather an overextended AVL axon. Note that the ectopic axons in *eno* mutants can derive from either the cell body (*eno-2* and *eno-3*, left) or the axon shaft (*eno-2* and *eno-3*, right). *eno-6* mutants show both ectopic axon branching (left) and axon misrouting (a premature termination is shown, right). *eno-7* also shows axon misrouting and axon branching (arrowheads). Both *eno-6* and *eno-7* and are shown in an *unc-30(e191)* mutant background to prevent D-type motor neurons from obscuring DVB anatomy. A dashed line indicates the location of the ventral nerve cord.

self-progeny for several generations. We reasoned that growing the animals for several generations before anatomic analysis would "dilute out" animals compromised in viability and brood size. We then analyzed these progeny on a population basis with a high-power compound fluorescence microscope specifically focusing on the tail region, which contains the axon terminus of AVL and the cell body of DVB (Figures 1 and 2).

Screening through ~5300 mutagenized haploid genomes, we isolated 12 mutants with anatomical defects of the AVL and/or DVB motor neurons, at least 10 of which define different complementation groups located in distinct chromosomal intervals (Figure 2; Table 1). On the basis of their axonal phenotypes, mutants were termed *eno* (*e*ctopic/*e*rratic *n*eurite *o*utgrowth of the AVL or DVB motor neurons). All *eno* mutants are viable, show an approximately normal brood size, and display normal locomotory behavior, with the exception of *ot2* animals, which are sluggish. All *eno* mutants are recessive, again with the exception of *ot2*, which is semidominant (data not shown). Two types of neuroanatomical defects of GABAergic neurons can be observed to a variable degree in *eno* mutants. One type of defect is characterized by what appears to be ectopic axons that emanate from the cell body or main axon shaft; the other type is characterized by the main axon of DVB and/or AVL straying off their normal path and/or terminating inappropriately (Figure 2; Table 1). We also isolated one mutant, *ot32*, which displayed cell shape defects reminiscent of those seen in *sax-1* mutant ani-

TABLE 1

Characterization of ectopic/erratic neurite outgrowth (*eno*) mutants

Mutant[a]	Map position	Nature of allele	Penetrance of axon defects[b]			
			% AVL/DVB axon (*n*)[c]	% D-type motor neurons (*n*)[c]	% amphid sensory axons (*n*)[d]	% AIY interneuron (*n*)[e]
eno-1/lin-23(ot1)	LGII, cloned	Recessive	73 (131)	wt	wt	wt
eno-3(ot3)[f]	LGX: −5.33 to −1.35	Recessive	41 (88)	wt	wt	ND
eno-4(ot4)[g]	LGII	Recessive	29 (52)	wt	wt	wt
eno-8(ot8)	LGIII: −1.46 to 0.0	Recessive	33 (27)	94 (50)	wt	wt
eno-9(ot9)[f]	LGX	Recessive	47 (114)	wt	wt	ND
eno-11(ot40)[h]	LGI: −5.6 to 0	Recessive	46 (114)	wt	34 (56)	wt
eno-2(ot2)[h]	LGI: −5.6 to +2.9	Semidominant	57 (92)	13 (46)	52 (62)	41 (32)
eno-6(ot6)[i]	LGV: 2.17 to 4.55	Recessive	35 (103)	wt	37 (41)	wt
eno-7(ot7)	LGIV	Recessive	36 (156)	wt	23 (31)	wt

[a] Mutants are grouped according to phenotypic categories. *eno-1*, *-3*, *-4*, *-8*, and *-9* affect only one class of neurons tested; *eno-11* affects two classes; while *eno-2* affects all classes tested. *eno-6* and *eno-7* show a qualitatively distinct defect, namely axon misrouting.

[b] wt, wild-type-like appearance; ND, not determined.

[c] Axon outgrowth or sprouting defects were scored at 25° using the *oxIs12* transgene. The defects in *ot2* and *ot8* classify as sprouting of the commissures. The defects in *ot6* and *ot7* are a sum of DVB sprouting and DVB misrouting defects. Wild-type animals show 0% defects ($n = 103$).

[d] Scored by staining with the lipophilic dye DiI. Defects classify either as axon misrouting (*ot6* and *ot7*) or as axon branches or sprouts derived from either the cell body or the main axon shaft (*ot40* and *ot2*). Wild-type animals show 7% background defects ($n = 41$).

[e] Scored with the *mgIs18* transgene. Defects classify as axonal branches or sprouts emanating from either the cell body or the main axon shaft. Wild-type animals show 6% background defects ($n = 50$).

[f] *ot9* complements *ot3*. *ot9* and *ot3* also complement *sax-1*.

[g] Complements *ot1*.

[h] *sax-6*, *ot2*, and *ot40* all complement each other. The semidominance of *ot2* complicates the interpretation of the complementation test.

[i] Complements *deg-3*, *des-2*, *flr-2*, and *vab-1*.

mals (Zallen *et al.* 2000). *ot32* maps to LGX but complements *sax-1*. We have not pursued a further characterization of this mutant.

The penetrance of the axonal defects in several of the *eno* mutants is significantly reduced by lowering the cultivation temperature to 15° (Figure 3A). This temperature sensitivity may reflect a temperature-sensitive nature of the mutant protein product or an underlying temperature sensitivity of the *eno* phenotype. The latter case would be supported by the observation that null alleles of genes affecting neuronal activity show temperature-sensitive axon sprouting defects (Peckol *et al.* 1999).

Since the GABAergic DVB and AVL motor neurons mediate the expulsion step of the defecation motor program, we next examined whether abnormal axon outgrowth of DVB or AVL in *eno* mutants would affect the functional output of these neurons. We found that *eno-2(ot2)*, *eno-4(ot4)*, *eno-7(ot7)*, *eno-8(ot8)*, *eno-9(ot9)*, and *eno-11(ot40)* show expulsion defects, which are weaker than the defects observed in GABA-deficient *unc-25* mutants (Figure 3B). The moderate nature of the defects and the lack of significant defects in *eno(ot1)*, *eno-3(ot3)*, and *eno-6(ot6)* may be explained by *eno* mutants differentially affecting DVB and AVL, both of which have a redundant function in regulating enteric muscle contractions (McIntire *et al.* 1993; *e.g.*, as we show below, *eno(ot1)* affects only AVL but not DVB axon outgrowth). Alternatively, ectopic axon outgrowth may have no impact on synapse formation and neuron function.

Other nervous system defects in *eno* mutants: To survey the extent of neuroanatomical defects in the *eno* mutants, we visualized several classes of neurons with a panel of *gfp* reporter genes as well as by dye filling. We observed defects in the morphology of D-type motor neurons in *eno-2(ot2)* and *eno-8(ot8)*, which display axon sprouting defects in the commissural axon tracts (Figure 4; Table 1; data not shown). Amphid sensory neurons, which were visualized with the lipophilic dye DiI, displayed defects in *eno-2(ot2)*, *eno-6(ot6)*, *eno-7(ot7)*, and *eno-11(ot40)*, but not in any other *eno* mutant (Figure 4; Table 1). The amphid sensory neuron defects fall into two different categories. *eno-2(ot2)* and *eno-11(ot40)* display amphid axon sprouting defects, whereas *eno-6(ot6)* and *eno-7(ot7)* display ASJ axon guidance defects, such that the main ASJ axon fails to extend appropriately along the normal route taken by amphid sensory axons (Figure 4; Table 1).

Amphid axon sprouting defects have been observed in some of the *sax* mutants (***s**ensory **ax**on defective*), namely

A

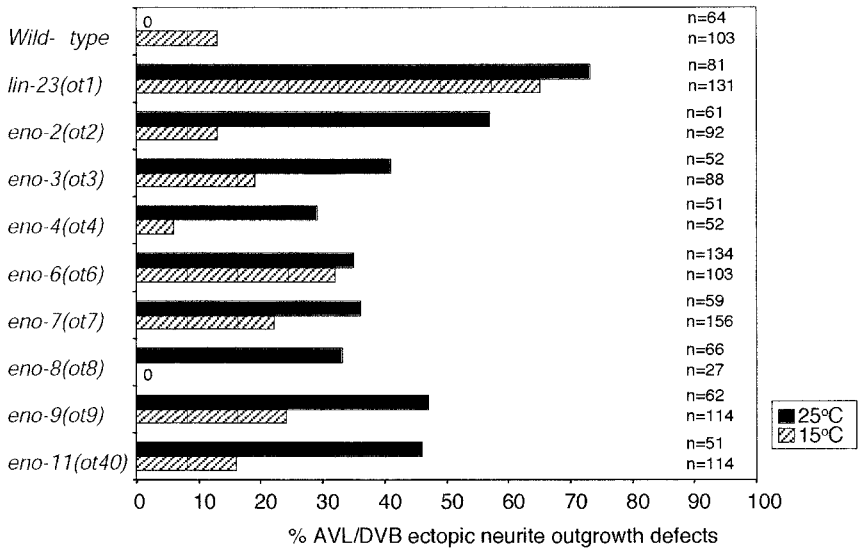

B

% intact EMC	*Wild-type*	*lin-23 (ot1)*	*eno-2 (ot2)*	*eno-3 (ot3)*	*eno-4 (ot4)*	*eno-6 (ot6)*	*eno-7 (ot7)*	*eno-8 (ot8)*	*eno-9 (ot9)*	*eno-11 (ot40)*	*unc-25 (e156)*
100	******* ***	***** *****	*****	*****	**	***** ****	***** *	*	****** **	**	
80			**		*	*	*	**		**	
60			**		*		*				
40							*	**	**		
20			*		*		*			*	****
0											******
Total # expulsion cycles	75	50	25	25	25	50	50	25	50	25	50

FIGURE 3.—Characterization of GABAergic neuronal defects in *eno* mutants. (A) The *eno* phenotype of several *eno* mutants is temperature dependent. AVL/DVB axon defects were scored with *oxIs12*. (B) The *eno* mutants show normal to moderately defective defecation behavior. Five to 10 defecation cycles were scored for each genotype at 25°. Each asterisk represents a single animal. EMC, enteric muscle contractions.

sax-1, *sax-2*, and *sax-6* (ZALLEN *et al.* 1999). We found that these three *sax* mutants also yielded an *eno* phenotype in the AVL and DVB motor neurons [penetrance: *sax-1 (ky211)*, 58%, $n = 41$; *sax-2(ky216)*, 95%, $n = 93$; *sax-6 (ky214)*, 35%, $n = 37$]. Mapping and complementation data indicate that *eno* and *sax* genes define distinct loci (Table 1).

After analyzing motor neurons (AVL, DVB, and D-type) and sensory neurons (amphid neurons), we next examined interneuron anatomy using a cell-type-specific marker for the AIY interneuron class (*ttx-3::gfp*). We found that *eno-2(ot2)* but no other examined *eno* mutant displayed an interneuron axon sprouting phenotype (Figure 4; Table 1). Further extending our analysis of *eno-2(ot2)*, we found that all other examined neuron classes (ASE chemosensory, mechanosensory, and SAB motor neurons) also displayed axon sprouting defects (data not shown).

Taken together, the *eno* mutants fall into different categories. One category affects axonal outgrowth of a subset of neurons [*eno(ot1), eno-3(ot3), eno-4(ot4), eno-8(ot8), eno-9(ot9)*, and *eno-11(ot40)*] and another category affects all neuron classes tested [*eno-2(ot2)*]. Mutants in both categories have axons and dendrites that take their correct path, but either fail to terminate appropriately or extend additional, aberrant axon sprouts. In contrast, mutants in the last category [*eno-6(ot6)* and *eno-7(ot7)*] display axonal sprouts as well as axon pathfinding defects of their main axon.

We chose to pursue a more detailed cellular and molecular characterization of the *ot1* allele due to its highly penetrant *eno* phenotype in the GABAergic neurons and due to its apparent cell-type specificity.

***eno(ot1)* affects axon outgrowth and targeting of specific classes of sensory and motor neurons:** *eno(ot1)* mutant animals display a GABAergic axon outgrowth defect, characterized by an overextended axon that can be detected in the posterior end of the animal; this

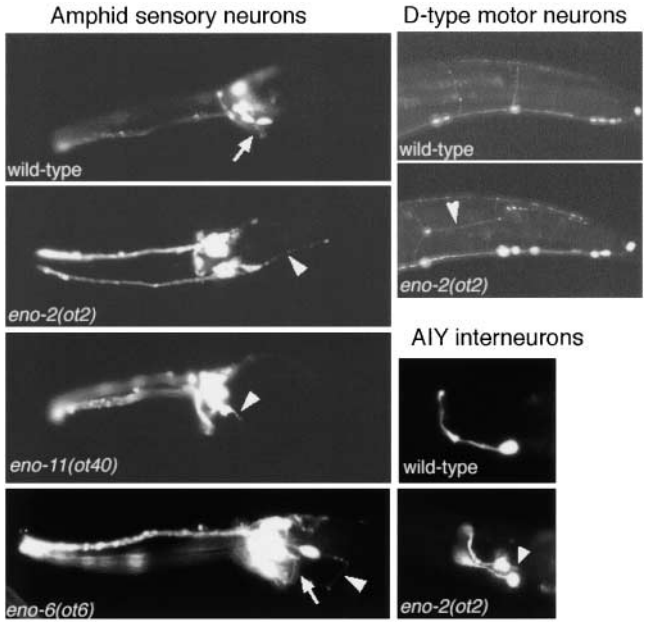

Figure 4.—Additional neuroanatomical defects in *eno* mutants. Anatomy of head amphid sensory neurons is visualized by DiI staining. *eno-2(ot2)* and *eno-11(ot40)* animals show ectopic axon sprouting defects (arrowhead). *eno-6(ot6)* shows an amphid axon misrouting defect, characterized by amphid axon(s) not being part of the amphid commissure (arrow). Similar defects are seen in *eno-7(ot7)* (not shown). Anatomy of the D-type motorneurons is visualized with the *oxIs12* transgene and AIY interneuron anatomy is visualized with the *mgIs18* transgene. Aberrant sprouting is indicated with an arrowhead. *eno-2(ot2)* shows ectopic outgrowth of axons from either the cell body of AIY (arrowhead) or the main axon shaft (not shown).

aberrantly extended axon also often displays ectopic branches (Figures 2 and 5A). The overextended axon can be an inappropriately terminated AVL motor axon or an inappropriately terminated D-type motor axon or may be an ectopic sprout derived from the DVB motor neuron. To distinguish among these possibilities, we genetically eliminated the D-type motor neurons using an *unc-30(e191)* mutant background (Jin *et al.* 1994; Eastman *et al.* 1999) and found that the appearance and penetrance of *eno(ot1)* outgrowth defects remains the same in *eno(ot1)* and *eno(ot1);unc-30(e191)* animals (Figure 5B, data not shown). Thus, the overextended axon in *eno(ot1)* animals cannot derive from D-type ventral cord neurons. The *eno(ot1); unc-30(e191)* strain also allowed us to score termination of the DVB axon at the vulva, which we found to be unaffected. In addition, we observed no DVB axonal defects upon visualization of DVB with a *gfp* transgene that is expressed in DVB but not in AVL (*otIs92*). We conclude that the axon termination defect in *eno(ot1)* can be assigned to the AVL motor neuron. Consistent with the notion of defective termination of axon outgrowth, we furthermore note that the outgrowth of the AVL axon continues through larval stages, resulting in a more penetrant mutant phenotype in adult animals compared to young larvae (data not shown).

As described above, *eno(ot1)* mutants do not display defects in DVB motor neuron, amphid sensory neuron, or AIY interneuron morphology. We further extended our analysis of neuroanatomical defects in *eno(ot1)* mutants by crossing *eno(ot1)* mutant animals with transgenic *gfp* reporter strains that label additional sets of sensory, inter-, and motor neurons (Figure 1). We found no defects in the axon anatomy of ASE chemosensory neurons or PVQ ventral cord interneurons (data not shown). However, we found that SAB head motor neurons show multiple defects in *eno(ot1)* mutants including ectopic sprouting from the axon, misrouting of the neuron from its original path, and an overgrowth of the axon, that is, a failure to terminate outgrowth appropriately (Figure 5A). Mechanosensory axons also fail to terminate outgrowth, an effect that is strictly temperature dependent (Figure 5A).

The appropriate expression of several *gfp*-marked genes (*unc-47, mec-18*, and *unc-4*) suggests that execution of cell fate is normal in *eno(ot1)* mutants. Hence, the axon outgrowth and pathfinding defects observed using these markers may represent a direct consequence of defective axon outgrowth machinery rather than a consequence of inappropriate execution of cell fate.

***ot1* is an allele of *lin-23*:** Through a combination of multifactor, single-nucleotide polymorphism-based mapping and deficiency analysis, we localized the *eno(ot1)* locus to a 62-kb region on chromosome II. This region contains the previously described *lin-23* locus. Complementation tests (not shown), transformation rescue (Figure 6), and allele sequencing (Figure 7A) demonstrated that *ot1* is allelic to the *lin-23* locus. From here on, we refer to *eno(ot1)* as *lin-23(ot1)*. *lin-23* was previously shown to encode an F-box protein with WD40 repeats that is a component of SCF-type E3 ubiquitin ligase complexes (Figure 7C; Kipreos *et al.* 2000). In comparison to its vertebrate, fly, and yeast orthologs, the predicted LIN-23 protein has a significantly extended C terminus (>100 amino acids; Figure 7A). *ot1* is a missense mutation leading to a single-amino-acid change (proline 610 to serine) within the nonconserved C-terminal tail (Figure 7, A and B). Proline 610 lies in a motif of the protein (PAPP) that constitutes a potential binding site (PXXP) for SH3 domain or WW domain containing protein ligands (Macias *et al.* 2002), suggesting that in *ot1* mutants a specific protein interaction of LIN-23 may be disrupted (Figure 7C). To corroborate this notion, we examined whether the extended C-terminal tail of *C. elegans* LIN-23 and its PAPP motif is conserved in the *C. briggsae* ortholog of LIN-23. The recently released genome sequence of *C. briggsae* contains a single LIN-23 ortholog, which is 89% identical to *C. elegans* LIN-23. The C termini of the two proteins, however, are highly diverged, yet the PAPP motif is completely conserved (Figure 7B). The conservation of this motif

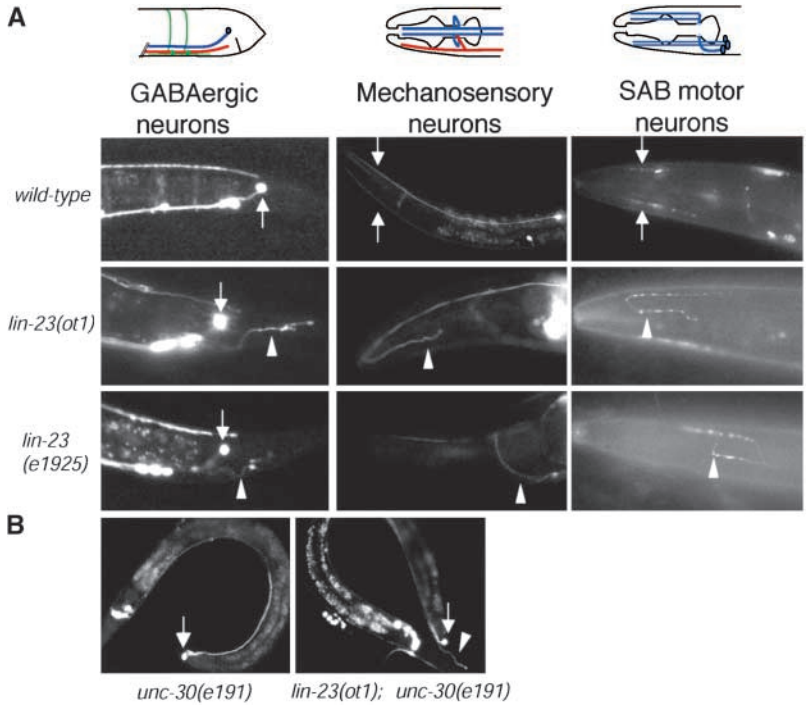

FIGURE 5.—Axon outgrowth defects in *eno(ot1)* mutant animals. (A, left) The AVL axon (red) travels along the ventral cord and terminates just before the DVB cell body (blue; arrow). AVL overgrowth defects are denoted by arrowheads. (Middle) Touch sensory neurons ALM (blue) and AVM (red) normally extend their axons toward the tip of the nose (arrows). All *lin-23* alleles show outgrowth defects including a failure of AVM to terminate appropriately (middle arrowhead) or a failure to extend past the nerve ring (bottom arrowhead). The defects of the *ot1* mutant allele in the touch neurons can be observed only at 25°. (Right) SAB motor neurons, which normally terminate in the tip of the nose (arrows), show outgrowth defects (arrowheads) in *lin-23* mutants. (B) Overextended GABAergic tail axons in *ot1* mutants derive from the AVL motor neuron (arrowhead). Animals carry the *unc-30(e191)* mutation and the *oxIs12* transgene. The *unc-30(e191)* allele eliminates *oxIs12*-conferred *gfp* expression in the D-type motor neurons of the ventral cord (JIN *et al.* 1994; EASTMAN *et al.* 1999).

within a region of little overall homology underscores the functional relevance of this motif.

We next tested the effect of previously isolated *lin-23* alleles, most of which are likely null alleles (KIPREOS *et al.* 2000), on axon outgrowth. Using *gfp* markers for the GABAergic motor neurons, touch neurons, and SAB-type motor neurons, we found that all other known *lin-23* alleles also affected axon anatomy of these neuron classes (Figures 5A and 9). The cell-type specificity also appears to be the same; that is, cell types that were not affected in *ot1* mutants (amphid sensory neurons) were also not affected in *lin-23* null mutants. Furthermore, the GABAergic and SAB motor neuron defects are qualitatively and quantitatively indistinguishable between *ot1* and previously described null alleles (Figures 5A and 9, A and C). In contrast, however, the defects of the mechanosensory neurons appear different. The putative *lin-23* null alleles cause the mechanosensory axons to leave their appropriate track, while the *ot1* mutation affects only the axon termination site rather than the track taken by the neuron (Figures 5A and 9B).

The neuroanatomical defects of *lin-23* null mutants in the AVL neuron and the touch sensory neurons are not accompanied by behavioral defects in enteric muscle contractions (regulated by AVL and DVB), anterior body wall muscle contraction (regulated by AVL only),

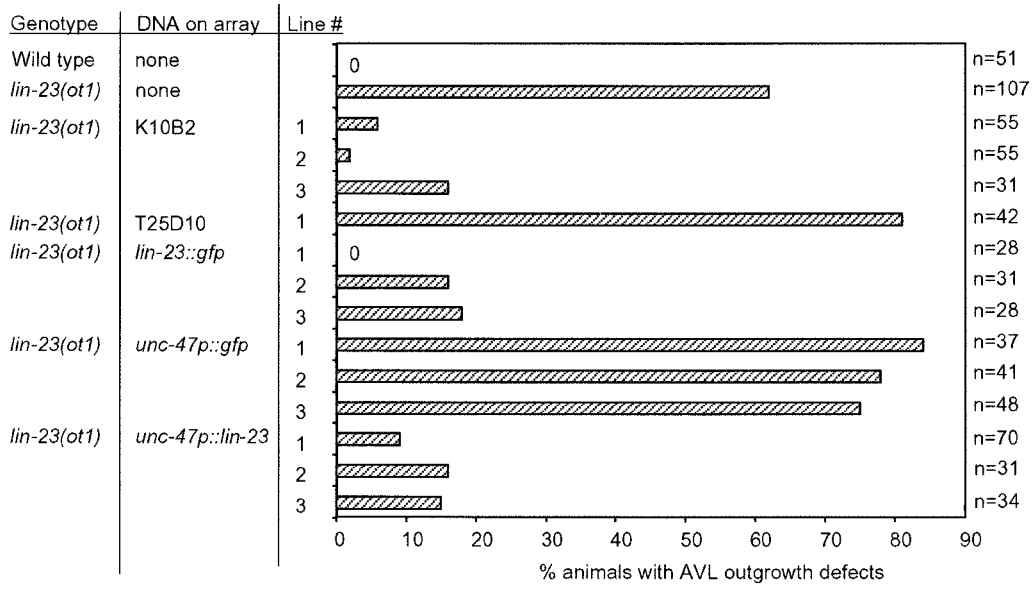

FIGURE 6.—*ot1* is an allele of *lin-23*. Transformation rescue experiments are shown. K10B2 is a cosmid that contains the *lin-23* gene as well as four other predicted genes. T25D10 is an unrelated control cosmid that neighbors K10B2. *lin-23::gfp* is a translational fusion of the *lin-23* locus to *gfp*. *unc-47p* is a GABAergic neuron-specific promoter that was injected either as a fusion with *lin-23* or with a control sequence (*gfp*). All DNA was injected at 20 ng/μl with *rol-6(d)* as an injection marker.

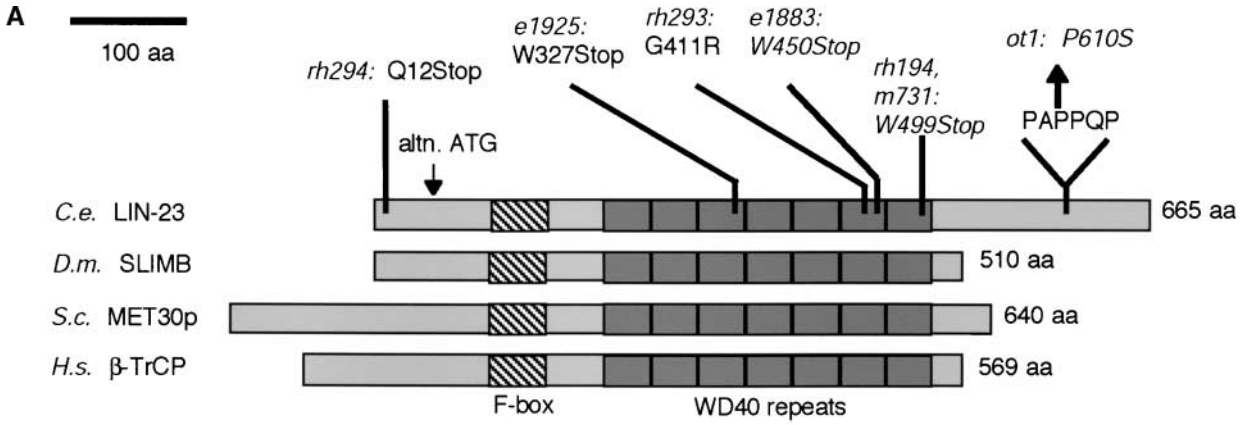

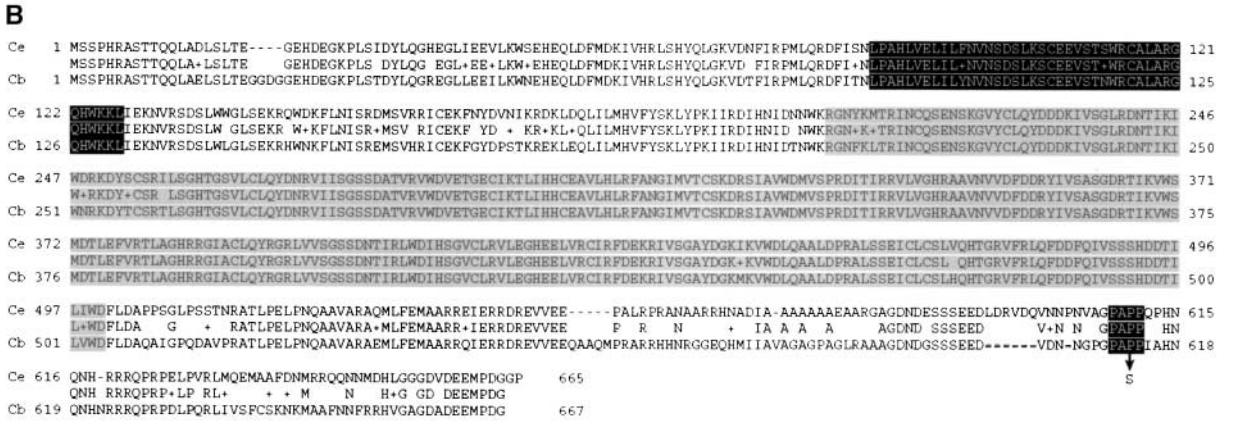

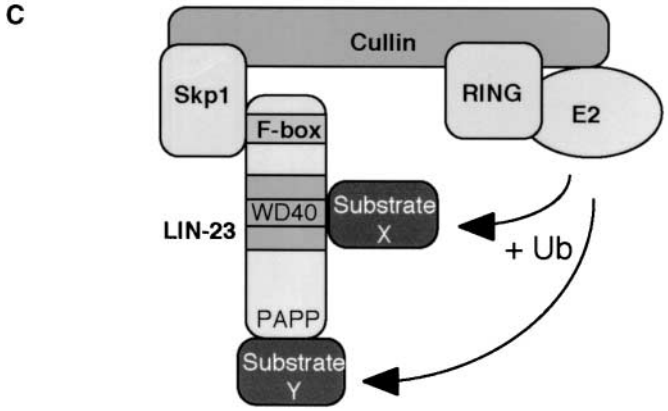

FIGURE 7.—LIN-23 structure and alleles. (A) LIN-23, its mutant alleles, and orthologous proteins are shown. The molecular nature of *m731* has not been described before. The *ot1* allele affects a proline in a predicted SH3/WW domain binding site (PAPP). All other mutant alleles have previously been described by KIPREOS *et al.* (2000). (B) The PAPP motif is conserved in the *C. briggsae* ortholog of LIN-23. The F-box at the N terminus is boxed in black; the seven consecutive WD40 repeats are shaded in gray; and the PAPP motif, located in the otherwise highly divergent C terminus, is boxed in black. The P610S mutation in *ot1* is indicated by an arrow. (C) SCF-type E3 ubiquitin ligase complexes. Structural studies revealed that cullin serves as a bridge to bring together different components of the complex (ZHENG *et al.* 2002). Substrates are recruited by protein-protein interaction domains (in this case, WD40 domains) of the F-box protein, while the F-box recruits other components of the ligase complex. We speculate that the PAPP motif is involved in recruiting a set of substrate(s) required for axon outgrowth while it has no role in recruiting substrates involved in cell cycle control; those may be recruited by the WD40 repeats.

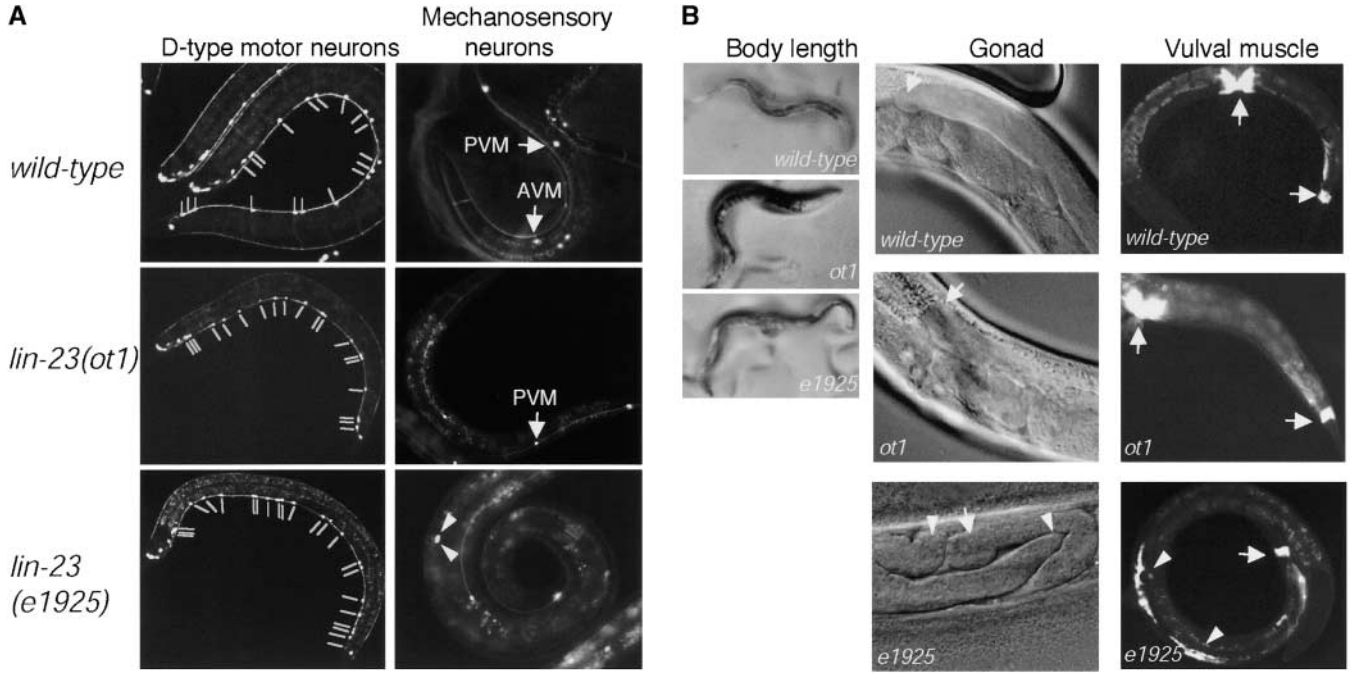

FIGURE 8.—Cellular proliferation defects in *lin-23* mutants. (A) Neuronal proliferation defects in *lin-23* mutants. (Left) Effect of *lin-23* alleles on ventral cord D-type motor neurons, visualized with the *oxIs12* transgene (cell bodies are labeled with gray lines). Six D-type neurons, the DD neurons, are embryonically generated, while 13 D-type neurons, the VD neurons, are postembryonically generated. (Right) Effect of *lin-23* alleles on touch sensory neurons, visualized with the *uIs25* transgene. Wild-type, postembryonically generated sensory cell bodies are shown with arrows and ectopic cell bodies in a representative example are indicated with arrowheads. *lin-23(e1925)* animals show proliferation defects in AVM, PVM, and also PLM. A quantification of the defects is shown in Figure 9. (B) Nonneuronal proliferation in *lin-23* mutants. (Left) The overall body morphology and appearance of *ot1* mutant animals are indistinguishable from those of wild-type animals. In contrast, animals harboring canonical *lin-23* null alleles, such as *lin-23(e1925)*, are elongated and pale. (Middle) *ot1* animals display no distal tip cell (arrows) proliferation defects or ectopic gonad arms (arrowheads) as observed in *e1925* animals (bottom and KIPREOS *et al.* 2000). (Right) The proliferation and migration of postembryonically generated sex muscles are affected in canonical *lin-23* alleles (bottom, inappropriately proliferating sex myoblasts are scattered along the body, indicated with arrowheads), but not in *ot1* mutant animals. Sex muscles were visualized with a *ceh-24::gfp* reporter transgene (HARFE and FIRE 1998), *nuIs63*, which also labels enteric muscle in the tail of the worm (arrows).

or touch sensation (regulated by the six touch neurons; data not shown). An inability of an axon to appropriately terminate axon outgrowth may therefore not affect its normal patterns of neuronal connectivity and function. In this context, it is important to keep in mind that in *C. elegans* synapses are made *en passant*, rather than at axon termini (WHITE *et al.* 1986).

***ot1* separates axonal function from a cell cycle function of *lin-23*:** Previously described *lin-23* null mutant animals are characterized by an overproliferation of various postembryonically generated cell lineages leading to an elongated appearance and sterility of the animals (KIPREOS *et al.* 2000). These previous studies on *lin-23* cell proliferation defects have largely relied on observing cell lineages with Nomarski optics. However, it was not clear whether ectopic cells produced by cell cycle defects would be able to differentiate appropriately. We addressed this question by analyzing the fate of postembryonically generated lineages with neuronal cell-type-specific *gfp* reporter strains (Figure 1). The GABAergic neuron marker *unc-47::gfp (oxIs12)* labels the postembryonically generated VD and DVB motor neurons while the touch neuron marker *mec-18::gfp (uIs25)* labels the postembryonically generated AVM and PVM neurons (Figure 1). We found excessive fluorescent cell bodies in the postembryonically generated neuronal lineages examined in all except one of the previously described putative null alleles of *lin-23* (Figures 8A and 9; *rh294*, the exception, is described in more detail in the next section). We also found the embryonic PLM lineage to have cell proliferation defects in *lin-23* alleles. The *gfp* markers that we have used, a GABA transporter and a touch neuron-specific protein, can be classified as terminal differentiation markers. In spite of uncontrolled cell proliferation, the expression of terminal cell differentiation markers in ectopic neurons indicates that individual neuronal cell fates are still appropriately executed.

Intriguingly, the *ot1* allele, unlike all previously characterized *lin-23* alleles, displays no readily observable cell proliferation defects. *ot1* animals do not display the sterility or elongated appearance indicative of overproliferation of various tissues that is characteristic of previously described *lin-23* alleles (Figure 8B). No ectopic

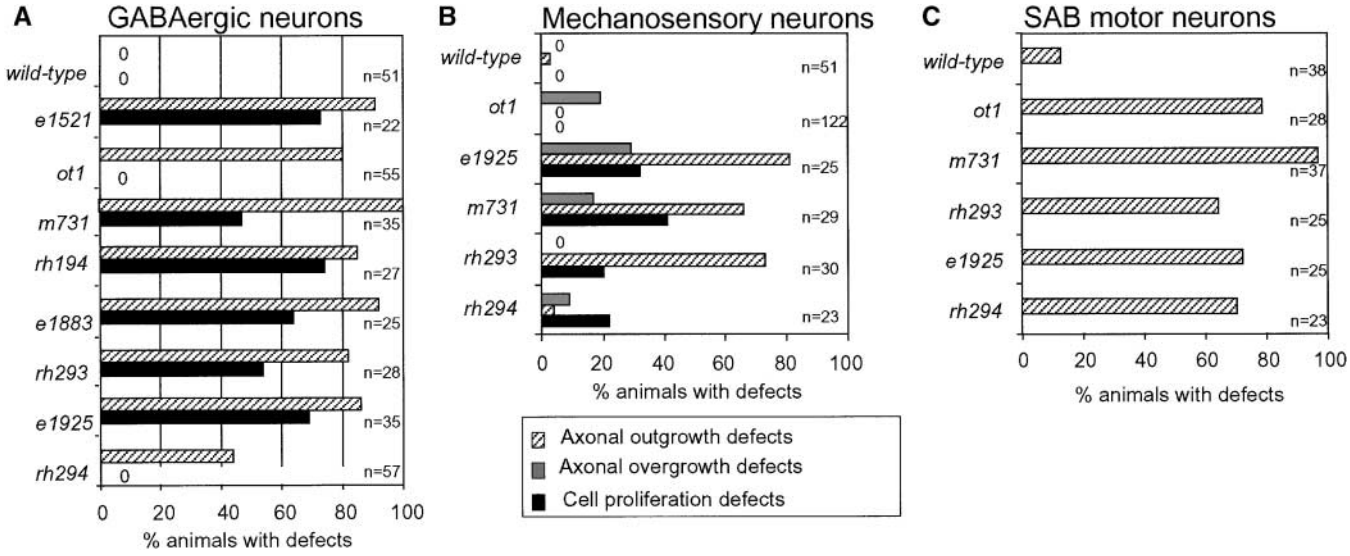

FIGURE 9.—Quantification of axonal defects and neuronal proliferation defects. (A) Quantification of effects of *lin-23* on D-type motor neuron proliferation and axon outgrowth. The wild-type number of D-type cell bodies was scored as 19 ± 1. Percentages of animals within a population that show defects are shown. An animal was scored as defective if it contained >20 cell bodies; up to 25 cell bodies were observed. Axon outgrowth defects refer to DVB and AVL axons. (B) Quantification of touch neuron defects (scored with *uIs25*). Axon outgrowth defects subsume wandering and premature termination (hatched bars). Axon overgrowth, *i.e.*, failure to terminate can be observed only in the ALM touch neuron (shaded bars). The touch neuron cell proliferation defects are a sum of those observed in AVM, PVM, and PLM. (C) Quantification of SAB motor neuron defects (scored with *jsIs42*). Axon outgrowth defects include wandering, sprouting, and overgrowth.

neuronal D-type motor neuron or touch neuron cell bodies were observed in *ot1* mutants (Figures 8A and 9). Moreover, no obvious proliferation defects are apparent in two types of nonneuronal tissue that we specifically examined, the distal tip cells and the postembryonically generated sex muscles; both cell types are affected by the *lin-23* null alleles (Figure 8B; KIPREOS *et al.* 2000). Lowering the dosage of *lin-23(ot1)* by placing this allele over a chromosomal deficiency that eliminates *lin-23*, *mnDf30*, also causes no proliferation defects, but recapitulates the axonal outgrowth defects (data not shown). Furthermore, *lin-23(ot1)* rescues the sterility of *lin-23* deficiency.

The lack of cell proliferation defects in *lin-23(ot1)* animals is in striking contrast to the observed axon outgrowth defects, which show a similar severity and cell-type specificity in *ot1* and *lin-23* null mutant animals. The absence of cell proliferation defects in *ot1* mutants also eliminates the possibility that the aberrant axons that we observe in all *lin-23* mutant alleles derive from aberrantly proliferated and hence possibly "confused" neurons. Taken together, these results suggest that LIN-23 has separable functions in cell cycle control and axon outgrowth (Figure 7C).

LIN-23 is a broadly expressed cytoplasmic protein: As a first step toward delineating the site of *lin-23* action, we examined its expression pattern. RNA *in situ* analysis demonstrated broad embryonic expression of *lin-23*, but lacked cellular resolution (KIPREOS *et al.* 2000). To analyze the expression pattern in more detail, we generated two *gfp* reporter gene constructs, one in which 2.2 kb of the 5′ upstream regulatory region of *lin-23* is fused to *gfp* (*lin-23prom::gfp*) and one in which the exons and introns of the gene are included (*lin-23::gfp*; Figure 10A). The *lin-23::gfp* construct completely rescues the mutant phenotype (Figure 6). Both constructs show similar expression patterns. Broad and possibly ubiquitous expression is first visible during gastrulation. Postembryonically, LIN-23 reporter fusions are expressed in many but not all neurons (*e.g.*, no expression is observed in commissural motor neurons), in body wall and enteric muscles, and in hypodermal cells (Figure 10B). The fusion protein is excluded from the nucleus and is uniformly distributed throughout the cytoplasm (Figure 10B). The protein also shows uniform distribution along axons (Figure 10B). LIN-23 expression is maintained in all tissues throughout adulthood. Given the absence of somatic cell divisions in adulthood, this observation is consistent with a role of LIN-23 that goes beyond cell cycle control in the developing organism and may hint at further roles of LIN-23 in fully differentiated cells.

The LIN-23::GFP rescuing construct provided us with an assay to test the stability and localization of *lin-23* mutant alleles. By introducing the *ot1* mutation (P610S) into the LIN-23::GFP construct (Figure 10A), we asked whether this mutation may potentially destabilize or mislocalize the protein. We found that LIN-23^{P610S}::GFP animals looked indistinguishable from LIN-23::GFP animals (Figure 10, B and C), consistent with our hypothesis that *ot1* has no gross effects on LIN-23 function but

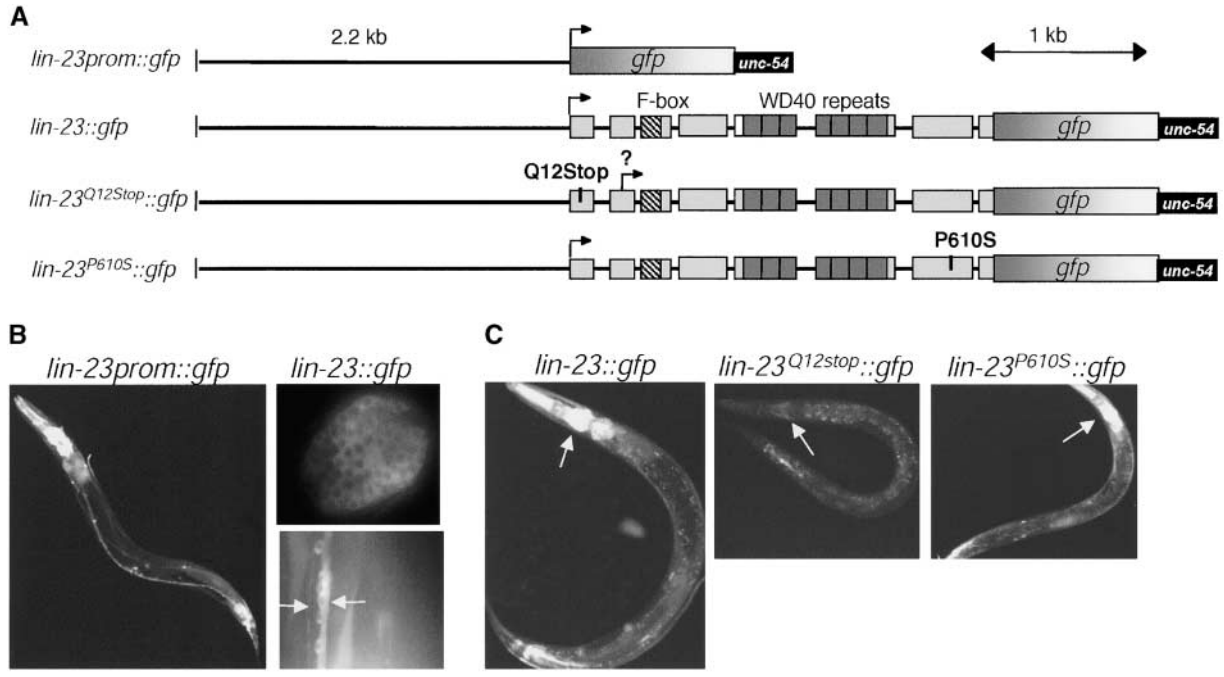

FIGURE 10.—LIN-23 is a broadly expressed cytoplasmic protein. (A) Schematic of expression constructs. Q12Stop corresponds to the mutation in the *rh294* allele and P610S to the *ot1* allele. A question mark indicates potential alternative start codons. (B) Expression of the *lin-23* transcriptional reporter (*lin-23prom::gfp*) and a *lin-23* translational reporter (*lin-23::gfp*). LIN-23::GFP first reveals expression during gastrulation and is strictly restricted to the cytoplasm in embryonic cells and throughout the cell body and axon in the ventral cord (arrows point to left and right cord) in adult animals. (C) Comparison of expression of wild-type and mutated forms of LIN-23::GFP in an adult wild-type background [slightly twisted due to the *rol-6(d)* injection marker]. All constructs were injected at the same concentration (20 ng/μl). At least three lines were scored per construct. Speckles are gut autofluorescence. Arrows point to expression in head ganglia.

may affect only its interaction with a specific subset of target proteins. It is possible, however, that a destabilizing effect of the P610S mutation may be compensated through the addition of the GFP moiety.

The *rh294* mutation, which was originally proposed to be a null allele, is an early stop codon 12 amino acids past the start site (KIPREOS *et al.* 2000). In contrast to the other putative *lin-23* null alleles, we found that *rh294* mutant animals affected the proliferation of touch neurons, but not of the VD ventral nerve cord motor neurons; axon outgrowth is also less severely affected in *rh294* animals (Figure 9). The hypomorphic nature of defects observed in *rh294* indicated that a more downstream start site may be used in these animals (*e.g.*, a methionine at position 56 or 78, both of which are still upstream of the F-box; Figure 10A). To test this notion we introduced the *rh294* mutation into the LIN-23::GFP fusion construct to create LIN-23^{Q12Stop}::GFP (Figure 10A). LIN-23^{Q12Stop}::GFP shows appreciable, though largely reduced expression levels (Figure 10C). The cellular and subcellular sites of expression appear unaffected.

***lin-23* acts cell autonomously in GABAergic neurons to affect axon outgrowth:** Defects in axon termination of the AVL motor neuron in *lin-23* mutants may be caused through defects in the neuron itself or in its synaptic target cells (for example, the enteric muscles), which may fail to provide an appropriate stop signal for the innervating neuron. To determine the focus of *lin-23* action, we expressed a *lin-23* cDNA under the control of the 5′ regulatory region of the *unc-47* gene, which is exclusively expressed in the GABAergic neurons including AVL (MCINTIRE *et al.* 1997). We find that *lin-23* is required cell specifically within the GABAergic neurons to rescue the AVL outgrowth defects and conclude that the gene acts cell autonomously (Figure 6).

Examination of other ubiquitin ligases in the nervous system: F-box proteins recruit protein substrates to SCF-type ubiquitin ligase complexes (Figure 7C). There are >300 F-box proteins in the *C. elegans* genome (KIPREOS and PAGANO 2000), yet only 2 of these F-box proteins, SEL-10 and T01E8.4, share a LIN-23-like domain composition of one F-box and several WD40 repeats. We asked whether SEL-10, the only one of the two LIN-23-like proteins for which mutant alleles are available (HUBBARD *et al.* 1997), may play a role in axonal development. We first examined those neurons whose morphology is not affected by LIN-23 (D-type motor neurons, DVB, and amphid sensory neurons) but found no defects in *sel-10(ar41)* null animals (data not shown). *sel-10* mutants also do not display defects in mechanosensory neurons, SAB motor neurons, or synaptic VAMP::GFP clustering within the GABAergic neurons. We conclude

that neurons that are unaffected by *lin-23* contain either another type of ubiquitin ligase or a mechanism independent of ubiquitination to ensure their correct axogenesis.

RING finger proteins constitute a different class of E3 ubiquitin ligases (Joazeiro and Weissman 2000), one example being Drosophila *highwire*, which is involved in synaptic signaling (Wan *et al.* 2000). Its worm ortholog *rpm-1* is, like *lin-23*, also a broadly expressed gene and shows a spectrum of mutant phenotypes that is remarkably similar to those of *lin-23*, specifically, touch neuron axon overgrowth and misrouting of SAB motor neurons (Schaefer *et al.* 2000; Zhen *et al.* 2000). We expanded the comparison of mutant phenotypes of *rpm-1* and *lin-23* and found that, unlike *lin-23* mutants, *rpm-1* mutants show no AVL overgrowth defects, but display DVB axon sprouting (data not shown). Furthermore, we found that *lin-23* mutants do not show the presynaptic VAMP::GFP clustering defects in GABAergic ventral cord motor neurons that are observed in *rpm-1* mutants (Schaefer *et al.* 2000; Zhen *et al.* 2000; data not shown). We conclude that different types of E3 ubiquitin ligase have some overlapping but also distinct functions in neuronal development.

DISCUSSION

***eno* mutants may define proteins involved in cell-specific aspects of axon guidance:** We have described here mutants retrieved from a forward genetic screen that display axon outgrowth defects in the AVL and DVB motor neuron classes. Mutants defective in DVB morphology display ectopic outgrowth defects from the axon or cell body. Several of the *eno* mutants also show axon sprouting defects in sensory and interneurons.

Ectopic axon outgrowth can be indicative of a failure to establish a functional connection of a neuron with its target cell (Brown *et al.* 1981; Zhao and Nonet 2000; Loria *et al.* 2003). Hence, *eno* mutants could affect steps relating to target recognition, synapse formation, or synaptic or retrograde signaling. *eno* mutants do not show defects normally associated with broadly acting synaptic transmission mutants, such as aldicarb resistance or uncoordinated locomotion (data not shown), and at least some of them show only a very restricted set of neuroanatomical defects. This may simply be an indication of a hypomorphic nature of our available *eno* alleles or may indicate that *eno* mutants affect cell-specific aspects of axogenesis rather than broad aspects of neurotransmission.

Some of the *eno* mutants show not only axon branching defects but also axon extension, misrouting, and defasciculation defects. These defects also display cell-type specificity; for example, *ot6* and *ot7* affect DVB and ASJ axon routing and fasciculation within the amphid commissure and ventral cord, but not AIY axon guidance and *lin-23(ot1)* displays AVL, but not DVB axon termination defects. Our genetic screen has thus defined a multitude of genes each affecting specific aspects of axogenesis in different cell types.

LIN-23, ubiquitin, and axogenesis: The *C. elegans* genome contains at least 326 predicted F-box proteins (Kipreos and Pagano 2000). Surprisingly, besides SEL-10, which regulates the degradation of LIN-12/Notch and SEL-12/presenilin (Hubbard *et al.* 1997; Wu *et al.* 1998), and FOG-2, an F-box protein involved in translational repression (Clifford *et al.* 2000), LIN-23 represents the only other *C. elegans* F-box protein for which a function has been reported. In addition to the previously documented role of *lin-23* in the cell cycle, we have described here a requirement for the *lin-23* gene in axon outgrowth of specific types of motor (AVL, but not DVB) and sensory neuron classes (touch neurons but not amphid neurons).

The AVL motor neuron axon normally makes several *en passant* synapses before it terminates in the preanal ganglion, where it makes synaptic contacts with preganglionic axons and the enteric muscles (White *et al.* 1986; Avery and Thomas 1997). In *lin-23* animals, the AVL axon takes a normal trajectory, but fails to terminate near the enteric muscles and instead overextends into the tail. These defects may be indicative of a failure of the axon to interpret a stop signal derived from one of its postsynaptic targets. When we genetically removed the enteric muscle target of AVL in *hlh-8* mutant animals (Corsi *et al.* 2000), we observed no AVL outgrowth defects (data not shown). Neurotransmission may also contribute in a negative feedback loop to the termination of axon outgrowth (Brown *et al.* 1981; Zhao and Nonet 2000), yet we have found that genetic removal of AVL's neurotransmitter, GABA, does not cause AVL overgrowth defects (data not shown). However, these data do not rule out the possibility that a complete and combined removal of all synaptic targets of AVL and/or a complete elimination of all synaptic transmission (GABA plus some unknown peptidergic transmission event; Loria *et al.* 2003) may impart a *lin-23*-like axon termination defect. It is also conceivable that axon stop signals are unrelated to the synaptic targets of a neuron and are rather presented by some distinct cellular source. No matter from where the stop signal is provided, the cell-autonomous function of *lin-23* in AVL prompts us to hypothesize that the reception and/or interpretation of this axon termination signal is disrupted in *lin-23* mutant animals.

A similar failure of axon termination is observed in the mechanosensory neurons of *lin-23* mutant animals. Interestingly, within the mechanosensory neuron context, an allelic series reveals differential defects based on severity of the *lin-23* mutation. These axons fail to follow the correct trajectory in strong loss-of-function *lin-23* alleles. However, in the *ot1* allele only the appropriate termination of axon outgrowth, but not the axonal trajectory, is affected. Yet a different scenario is observed in the SAB motor neurons. Here, all mutant

alleles show similar defects in choosing incorrect axon trajectories. The distinctiveness of axonal outgrowth defects observed in *lin-23* mutants in diverse cell types and with various mutant alleles may be caused by a distinct substrate spectrum of LIN-23 in different cell types. Alternatively, LIN-23 may affect a common set of substrates that function in a cellular context-dependent manner.

Our findings provide another example of the importance of ubiquitination in axon outgrowth, first recognized upon cloning of the *bendless* E2 ubiquitin ligase, which affects axon targeting in Drosophila (Muralidhar and Thomas 1993) and later corroborated by the implication of ubiquitination in Robo-mediated axon guidance at the fly midline (Myat *et al.* 2002). A new and intriguing aspect of our studies is the implication of *lin-23* in two distinct and genetically separable processes, cell cycle control *vs.* axonal development. The genetic separability of these two functions is consistent with several distinct possibilities. In one scenario, LIN-23 may act through a single target protein that controls both cellular processes and whose ubiquitination is differentially affected in *lin-23* null *vs. lin-23(ot1)* mutations. To our knowledge, there is only a single potential molecular link between cell cycle and axon outgrowth. The $p21^{Cip1/WAF1}$ protein, initially described as a nuclear inhibitor of the cyclin-Cdk kinase complex (Harper *et al.* 1993), has recently also been implicated in regulating neurite remodeling by inhibiting Rho-kinase activity in the cytoplasm (Tanaka *et al.* 2002). In an alternative scenario, LIN-23 may affect the ubiquitination of distinct targets that control different cellular processes (Figure 7C). One (set of) target(s) may be recognized through the extended C terminus, in which the *ot1* mutation is localized, affecting the ubiquitination of proteins required for axon outgrowth. Distinct binding sites for substrates involved in cell cycle control may be located within the WD40 repeats (Figure 7C). The multisubstrate scenario is consistent with the notion that the fly and vertebrate orthologs of LIN-23, termed Slimb and βTrCP, regulate the degradation of distinct components of Wingless, Hedgehog, and NFκB signaling pathways (Jiang and Struhl 1998; Yaron *et al.* 1998). Slimb has furthermore been implicated in a variety of cellular processes such as centrosome duplication (Wojcik *et al.* 2000), circadian timing (Grima *et al.* 2002; Ko *et al.* 2002), and transcriptional regulation (Heriche *et al.* 2003), further underscoring the distinct roles of a single ubiquitin ligase component.

In summary, we have provided here further evidence for the importance of ubiquitination in axon outgrowth. LIN-23 may cause ubiquitination of cell surface protein(s) required for axon guidance and target recognition. The failure to degrade or alter the subcellular targeting of such cell surface substrate(s) may lead to the axonal outgrowth defects observed in *lin-23* mutants. Alternatively, LIN-23 may have a more indirect impact on axon pathfinding through an involvement in ubiquitin-mediated, yet proteolysis-independent transcriptional regulation (Bach and Ostendorff 2003).

We thank Thomas Boulin, Stephane Conte, Ruby Hsu, Jane Rosen, Wendy Yip, and Jason Tien for their involvement in the genetic screens and mutant analysis; Mike Nonet, Josh Kaplan, and Erik Jorgensen for providing nematode strains; and Iva Greenwald and Edward Kipreos for comments on the manuscript. This work was funded by a grant from the National Institutes of Health (NIH; R01 NS 39996), the Muscular Dystrophy Association, and the Christopher Reeve Paralysis Association. O.H. is a Klingenstein, Rita Allen, Irma T. Hirschl, and Sloan Fellow. P.M.L was supported by an NIH postdoctoral fellowship (NS11144). N.M. was supported by NIH Molecular Aspects of Aging (T32 AG00289-12) and NIH Vision Sciences training grants (T32 EY 13933-01).

LITERATURE CITED

Altun-Gultekin, Z., Y. Andachi, E. L. Tsalik, D. Pilgrim, Y. Kohara *et al.*, 2001 A regulatory cascade of three homeobox genes, ceh-10, ttx-3 and ceh-23, controls cell fate specification of a defined interneuron class in C. elegans. Development **128:** 1951–1969.

Antebi, A., C. Norris, E. M. Hedgecock and G. Garriga, 1997 Cell and growth cone migrations, pp. 583–610 in *C. elegans II*, edited by D. L. Riddle, T. Blumenthal, B. J. Meyer and J. R. Priess. Cold Spring Harbor Laboratory Press, Cold Spring Harbor, NY.

Avery, L., and J. H. Thomas, 1997 Feeding and defecation, pp. 679–716 in *C. elegans II*, edited by D. L. Riddle, T. Blumenthal, B. J. Meyer and J. R. Priess. Cold Spring Harbor Laboratory Press, Cold Spring Harbor, NY.

Bach, I., and H. P. Ostendorff, 2003 Orchestrating nuclear functions: ubiquitin sets the rhythm. Trends Biochem. Sci. **28:** 189–195.

Bai, C., P. Sen, K. Hofmann, L. Ma, M. Goebl *et al.*, 1996 SKP1 connects cell cycle regulators to the ubiquitin proteolysis machinery through a novel motif, the F-box. Cell **86:** 263–274.

Brown, M. C., R. L. Holland and W. G. Hopkins, 1981 Motor nerve sprouting. Annu. Rev. Neurosci. **4:** 17–42.

Burbea, M., L. Dreier, J. S. Dittman, M. E. Grunwald and J. M. Kaplan, 2002 Ubiquitin and AP180 regulate the abundance of GLR-1 glutamate receptors at postsynaptic elements in C. elegans. Neuron **35:** 107–120.

Campbell, D. S., and C. E. Holt, 2001 Chemotropic responses of retinal growth cones mediated by rapid local protein synthesis and degradation. Neuron **32:** 1013–1026.

Clifford, R., M. H. Lee, S. Nayak, M. Ohmachi, F. Giorgini *et al.*, 2000 FOG-2, a novel F-box containing protein, associates with the GLD-1 RNA binding protein and directs male sex determination in the C. elegans hermaphrodite germline. Development **127:** 5265–5276.

Corsi, A. K., S. A. Kostas, A. Fire and M. Krause, 2000 Caenorhabditis elegans twist plays an essential role in non-striated muscle development. Development **127:** 2041–2051.

Craig, K. L., and M. Tyers, 1999 The F-box: a new motif for ubiquitin dependent proteolysis in cell cycle regulation and signal transduction. Prog. Biophys. Mol. Biol. **72:** 299–328.

DiAntonio, A., A. P. Haghighi, S. L. Portman, J. D. Lee, A. M. Amaranto *et al.*, 2001 Ubiquitination-dependent mechanisms regulate synaptic growth and function. Nature **412:** 449–452.

Eastman, C., H. R. Horvitz and Y. Jin, 1999 Coordinated transcriptional regulation of the unc-25 glutamic acid decarboxylase and the unc-47 GABA vesicular transporter by the Caenorhabditis elegans UNC-30 homeodomain protein. J. Neurosci. **19:** 6225–6234.

Grima, B., A. Lamouroux, E. Chelot, C. Papin, B. Limbourg-Bouchon *et al.*, 2002 The F-box protein Slimb controls the levels of clock proteins Period and Timeless. Nature **420:** 178–182.

Hammarlund, M., W. S. Davis and E. M. Jorgensen, 2000 Mutations in beta-spectrin disrupt axon outgrowth and sarcomere structure. J. Cell Biol. **149:** 931–942.

Harfe, B. D., and A. Fire, 1998 Muscle and nerve-specific regulation of a novel NK-2 class homeodomain factor in Caenorhabditis elegans. Development **125:** 421–429.

Harper, J. W., G. R. Adami, N. Wei, K. Keyomarsi and S. J. Elledge, 1993 The p21 Cdk-interacting protein Cip1 is a potent inhibitor of G1 cyclin-dependent kinases. Cell **75:** 805–816.

Hedgecock, E. M., J. G. Culotti, J. N. Thomson and L. A. Perkins, 1985 Axonal guidance mutants of Caenorhabditis elegans identified by filling sensory neurons with fluorescein dyes. Dev. Biol. **111:** 158–170.

Hedgecock, E. M., J. G. Culotti, D. H. Hall and B. D. Stern, 1987 Genetics of cell and axon migrations in Caenorhabditis elegans. Development **100:** 365–382.

Hegde, A. N., and A. DiAntonio, 2002 Ubiquitin and the synapse. Nat. Rev. Neurosci. **3:** 854–861.

Hegde, A. N., A. L. Goldberg and J. H. Schwartz, 1993 Regulatory subunits of cAMP-dependent protein kinases are degraded after conjugation to ubiquitin: a molecular mechanism underlying long-term synaptic plasticity. Proc. Natl. Acad. Sci. USA **90:** 7436–7440.

Hegde, A. N., K. Inokuchi, W. Pei, A. Casadio, M. Ghirardi *et al.*, 1997 Ubiquitin C-terminal hydrolase is an immediate-early gene essential for long-term facilitation in Aplysia. Cell **89:** 115–126.

Heriche, J. K., D. Ang, E. Bier and P. H. O'Farrell, 2003 Involvement of an SCFSlmb complex in timely elimination of E2F upon initiation of DNA replication in Drosophila. BMC Genet. **4:** 9.

Hicke, L., and R. Dunn, 2003 Regulation of membrane protein transport by ubiquitin and ubiquitin-binding proteins. Annu. Rev. Cell Dev. Biol. **19:** 141–172.

Hobert, O., 2002 PCR fusion-based approach to create reporter gene constructs for expression analysis in transgenic C. elegans. Biotechniques **32:** 728–730.

Hobert, O., K. Tessmar and G. Ruvkun, 1999 The Caenorhabditis elegans lim-6 LIM homeobox gene regulates neurite outgrowth and function of particular GABAergic neurons. Development **126:** 1547–1562.

Hochstrasser, M., 1996 Ubiquitin-dependent protein degradation. Annu. Rev. Genet. **30:** 405–439.

Hu, G., S. Zhang, M. Vidal, J. L. Baer, T. Xu *et al.*, 1997 Mammalian homologs of seven in absentia regulate DCC via the ubiquitin-proteasome pathway. Genes Dev. **11:** 2701–2714.

Huang, X., H. J. Cheng, M. Tessier-Lavigne and Y. Jin, 2002 MAX-1, a novel PH/MyTH4/FERM domain cytoplasmic protein implicated in netrin-mediated axon repulsion. Neuron **34:** 563–576.

Hubbard, E. J., G. Wu, J. Kitajewski and I. Greenwald, 1997 sel-10, a negative regulator of lin-12 activity in Caenorhabditis elegans, encodes a member of the CDC4 family of proteins. Genes Dev. **11:** 3182–3193.

Jiang, J., and G. Struhl, 1998 Regulation of the Hedgehog and Wingless signalling pathways by the F-box/WD40-repeat protein Slimb. Nature **391:** 493–496.

Jin, Y., R. Hoskins and H. R. Horvitz, 1994 Control of type-D GABAergic neuron differentiation by C. elegans UNC-30 homeodomain protein. Nature **372:** 780–783.

Joazeiro, C. A., and A. M. Weissman, 2000 RING finger proteins: mediators of ubiquitin ligase activity. Cell **102:** 549–552.

Keleman, K., S. Rajagopalan, D. Cleppien, D. Teis, K. Paiha *et al.*, 2002 Comm sorts robo to control axon guidance at the Drosophila midline. Cell **110:** 415.

Kipreos, E. T., and M. Pagano, 2000 The F-box protein family. Genome Biol. **1:** 3002.1–3002.7.

Kipreos, E. T., S. P. Gohel and E. M. Hedgecock, 2000 The C. elegans F-box/WD-repeat protein LIN-23 functions to limit cell division during development. Development **127:** 5071–5082.

Ko, H. W., J. Jiang and I. Edery, 2002 Role for Slimb in the degradation of Drosophila Period protein phosphorylated by Doubletime. Nature **420:** 673–678.

Loria, P. M., A. Duke, J. B. Rand and O. Hobert, 2003 Two neuronal, nuclear-localized RNA binding proteins involved in synaptic transmission. Curr. Biol. **13:** 1317–1323.

Macias, M. J., S. Wiesner and M. Sudol, 2002 WW and SH3 domains, two different scaffolds to recognize proline-rich ligands. FEBS Lett. **513:** 30–37.

McIntire, S. L., G. Garriga, J. White, D. Jacobson and H. R. Horvitz, 1992 Genes necessary for directed axonal elongation or fasciculation in C. elegans. Neuron **8:** 307–322.

McIntire, S. L., E. Jorgensen and H. R. Horvitz, 1993 Genes required for GABA function in Caenorhabditis elegans. Nature **364:** 334–337.

McIntire, S. L., R. J. Reimer, K. Schuske, R. H. Edwards and E. M. Jorgensen, 1997 Identification and characterization of the vesicular GABA transporter. Nature **389:** 870–876.

Muralidhar, M. G., and J. B. Thomas, 1993 The Drosophila bendless gene encodes a neural protein related to ubiquitin-conjugating enzymes. Neuron **11:** 253–266.

Murphey, R. K., and T. A. Godenschwege, 2002 New roles for ubiquitin in the assembly and function of neuronal circuits. Neuron **36:** 5–8.

Myat, A., P. Henry, V. McCabe, L. Flintoft, D. Rotin *et al.*, 2002 Drosophila Nedd4, a ubiquitin ligase, is recruited by Commissureless to control cell surface levels of the roundabout receptor. Neuron **35:** 447–459.

Nonet, M. L., 1999 Visualization of synaptic specializations in live *C. elegans* with synaptic vesicle protein-GFP fusions. J. Neurosci. Methods **89:** 33–40.

Peckol, E. L., J. A. Zallen, J. C. Yarrow and C. I. Bargmann, 1999 Sensory activity affects sensory axon development in C. elegans. Development **126:** 1891–1902.

Schaefer, A. M., G. D. Hadwiger and M. L. Nonet, 2000 rpm-1, a conserved neuronal gene that regulates targeting and synaptogenesis in C. elegans. Neuron **26:** 345–356.

Tanaka, H., T. Yamashita, M. Asada, S. Mizutani, H. Yoshikawa *et al.*, 2002 Cytoplasmic p21Cip1/WAF1 regulates neurite remodeling by inhibiting Rho-kinase activity. J. Cell Biol. **158:** 321–329.

Thomas, J. B., and R. J. Wyman, 1982 A mutation in Drosophila alters normal connectivity between two identified neurones. Nature **298:** 650–651.

Wan, H. I., A. DiAntonio, R. D. Fetter, K. Bergstrom, R. Strauss *et al.*, 2000 Highwire regulates synaptic growth in Drosophila. Neuron **26:** 313–329.

White, J. G., E. Southgate, J. N. Thomson and S. Brenner, 1986 The structure of the nervous system of the nematode *Caenorhabditis elegans*. Philos. Trans. R. Soc. Lond. B Biol. Sci. **314:** 1–340.

Williams, B. D., B. Schrank, C. Huynh, R. Shownkeen and R. H. Waterston, 1992 A genetic mapping system in Caenorhabditis elegans based on polymorphic sequence-tagged sites. Genetics **131:** 609–624.

Wojcik, E. J., D. M. Glover and T. S. Hays, 2000 The SCF ubiquitin ligase protein slimb regulates centrosome duplication in Drosophila. Curr. Biol. **10:** 1131–1134.

Wolf, B., M. A. Seeger and A. Chiba, 1998 Commissureless endocytosis is correlated with initiation of neuromuscular synaptogenesis. Development **125:** 3853–3863.

Wu, G., E. J. Hubbard, J. K. Kitajewski and I. Greenwald, 1998 Evidence for functional and physical association between Caenorhabditis elegans SEL-10, a Cdc4p-related protein, and SEL-12 presenilin. Proc. Natl. Acad. Sci. USA **95:** 15787–15791.

Wu, J., A. Duggan and M. Chalfie, 2001 Inhibition of touch cell fate by egl-44 and egl-46 in C. elegans. Genes Dev. **15:** 789–802.

Yamamoto, N., A. N. Hegde, D. G. Chain and J. H. Schwartz, 1999 Activation and degradation of the transcription factor C/EBP during long-term facilitation in Aplysia. J. Neurochem. **73:** 2415–2423.

Yaron, A., A. Hatzubai, M. Davis, I. Lavon, S. Amit *et al.*, 1998 Identification of the receptor component of the IkappaBalpha-ubiquitin ligase. Nature **396:** 590–594.

Zallen, J. A., S. A. Kirch and C. I. Bargmann, 1999 Genes required for axon pathfinding and extension in the C. elegans nerve ring. Development **126:** 3679–3692.

Zallen, J. A., E. L. Peckol, D. M. Tobin and C. I. Bargmann, 2000 Neuronal cell shape and neurite initiation are regulated by the ndr kinase SAX-1, a member of the Orb6/COT-1/Warts Serine/Threonine kinase family. Mol. Biol. Cell **11:** 3177–3190.

Zhao, H., and M. L. Nonet, 2000 A retrograde signal is involved in activity-dependent remodeling at a C. elegans neuromuscular junction. Development **127:** 1253–1266.

Zhen, M., X. Huang, B. Bamber and Y. Jin, 2000 Regulation of presynaptic terminal organization by C. elegans RPM-1, a putative guanine nucleotide exchanger with a RING-H2 finger domain. Neuron **26:** 331–343.

Zheng, N., B. A. Schulman, L. Song, J. J. Miller, P. D. Jeffrey *et al.*, 2002 Structure of the Cul1-Rbx1-Skp1-F boxSkp2 SCF ubiquitin ligase complex. Nature **416:** 703–709.

Communicating editor: P. Anderson